infrastructures

MDPI

Article

Experimental Study of the Mechanical Behaviour of Bricks from 19th and 20th Century Buildings in the Province of Zamora (Spain)

Ana Belén Ramos Gavilán [1,*], María Ascensión Rodríguez Esteban [2], María Natividad Antón Iglesias [2], María Paz Sáez Perez [3], María Soledad Camino Olea [4] and Julen Caballero Valdizán [2]

1 Mechanical Engineering Department, University of Salamanca, 49022 Zamora, Spain
2 Construction and Agronomy Department, University of Salamanca, 49022 Zamora, Spain; mare@usal.es (M.A.R.E.); nanton@usal.es (M.N.A.I); zandival@msn.com (J.C.V.)
3 Architectural Construction Department, University of Granada, 18071 Granada, Spain; mpsaez@ugr.es
4 Architectural Construction IT MMCC TE Department, University of Valladolid, 47014 Valladolid, Spain; mcamino@arq.uva.es
* Correspondence: aramos@usal.es; Tel.: +34-980545000-3728

Received: 31 July 2018; Accepted: 11 September 2018; Published: 16 September 2018

Abstract: Interventions in historic brick buildings require an exhaustive analysis of the current characteristics of bricks in order to establish the role performed by these elements in the buildings. This study presents the results of an experimental analysis of the compressive strength of brick specimens extracted from different buildings built in the 19th and 20th centuries in the province of Zamora (Spain). The study analyses specimens with very different characteristics to compare results from different masonry units and manufacturing processes. Specimens are classified into four groups according to their macroscopic and microscopic analyses. Compressive strength results are correlated to the above classification and to the results of density, absorption and open porosity of the samples. The compressive strength results present high variation between clay bricks (9.2–64.4 N/mm^2) and between samples extracted from the same brick due to the heterogeneity of the material. Correlations between compressive strength and open porosity, absorption and dry density values are observed, with less dispersion in the case of high sintering level, up to 1000 °C. Finally, the compliance with the current Spanish Technical Building Code with respect to their compressive strength is checked.

Keywords: compressive strength; historic bricks; restoration and rehabilitation

1. Introduction

Many studies on interventions in historical masonry buildings, such as those conducted by Binda et al. [1], Papayianni and Stefanidou [2], Lourenço and Fernandes [3], Brandonisio et al. [4] and Vintzileou [5], point to the importance of knowing the manufacturing conditions and the compressive strength, as well as the compatibility with other materials. The mechanical analysis of bricks is common in many of them, including the works of Fernandes and Lourenço [6], Singha, et al. [7], Matysek et al. [8], Balasubramanian et al. [9], Azeez et al. [10], Pérez-Gálvez et al. [11], Brozovsky et al. [12] and Bajare et al. [13]. Because of the difficulty of extracting samples, estimates of the bearing capacity of brick walls based on empirical formulas and analytical models that use the bricks and mortar strength are very useful. European Standard EN 1996-1-1 [14] and different research works, such as Sahlin [15] and Kaushik et al. [16], collect some of the most significant methods. Numerical models based on mechanical properties of the constituents reduce the difficulties associated with masonry laboratory tests. Computer

simulations can predict the mechanical behaviour and compressive strength of masonry buildings, as reported by Lemos [17], Barbosa et al. [18], Uday et al. [19] and Sousa [20].

This paper analyses the results of compressive strength tests carried out on ancient clay brick samples extracted from facades of different buildings built in the 19th and 20th centuries in the province of Zamora (Spain) during their intervention or demolition. The work includes the experimental analysis of the porosity, absorption and density, as well as the macroscopic and microscopic study of the material. The compression strength of clay bricks is related to their physical properties, origin and manufacturing process.

Lastly, the study checks on compliance with the requirements of BD SE-F of the Spanish Technical Building Code [21], which facilitates the evaluation of the state of conservation of the building, required by Law 8/2013 LRRRU [22].

2. Brick Specimens

This study was carried out on 15 ancient clay bricks from buildings located in different municipalities of the province of Zamora. The selected buildings were built between the end of the 19th century and the beginning of the 20th century. Most of them originate from Toro, where brick building construction greatly increased at the end of the 19th century, or were manufactured in the San Antonio Factory, located in the municipality of El Perdigón. The study also includes a clay brick from the municipality of Otero de Bodas, located in the Sanabria-La Carballeda Area, and another one from Entrala. Most of the clay bricks analysed were traditionally produced by a handmade process, except those manufactured in San Antonio Factory by extruded or moulded process. The clays used come from different facies, mainly from Entrala and Tierra de Campos. Therefore, the study analyses samples with different origins, manufacturing processes, surface finishes and physical properties.

Macroscopic and Microscopic Study

Prior to the mechanical analysis of bricks, an initial visual inspection and an optical microscopy analysis were carried out. This initial study facilitates the specimen description based on peculiarities: inclusions, phases, textures, flow lines caused by the manufacturing process, interaction between minerals, sintering and firing processes, reactions between particles, etc.

The analysed bricks are classified into four groups according to the visual inspection and their behaviour during the cutting process. Group number one (G1) is made up of bricks 1, 6 and 8. These specimens present soft zones detected by visual inspection and cutting process, which have yellowish colour because of the low content in iron oxides [23–30], and cracks between macro phases. A detail of one sample classified as G1 is shown in Figure 1a.

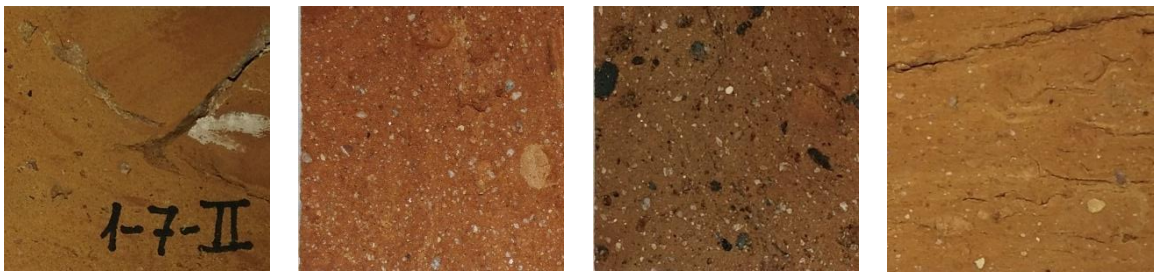

(**a**) (**b**) (**c**) (**d**)

Figure 1. Brick classification based on macroscopic analysis: (**a**) G1; (**b**) G2; (**c**) G3; (**d**) G4.

Bricks 2, 5, 7 and 9 form group number two (G2). The visual inspection of these bricks identify granular texture because of the sand particle content, as can be seen in Figure 1b.

Clay bricks 3, 4 and 10 form the third group (G3). These specimens present vitreous zones, identified by optical microscopy, and large visible purple and dark red areas identified by optical

microscopy and visual inspection. Clay bricks of this group present hardness when cut, and their optical microscopy analysis reveals a solid cohesion, since there are no necks between particles, the initial stage of sintering [31]. Figure 1c shows a brick sample classified as G3.

Finally, the fourth group (G4) is made up of moulded and extruded bricks manufactured in San Antonio Factory, which correspond to specimens 11 to 15. These bricks show flow lines due to the shaping process, as shown in Figure 1d, which could weaken some load directions.

Table 1 summarizes the main results obtained in the visual inspection and optical microscopy study of each specimen, with *T* representing the estimated firing temperature, *D* the disintegration or detachment of particles during the handling of the pieces, *R* the reaction between mineralogical components during firing, *Df* the silica diffusion and breakage after firing, *I* the final interaction between the clay minerals, and *C* the red colour due to the higher content of iron oxides. *D* and *C* are visually assessed, *R*, *Df* and *I* are identified by optical microscopy, and *T* is estimated through visual inspection and optical microscopy. Since the range of temperatures from 900 to 1000 °C is suitable for the firing/sintering of bricks, the presence of necks between particles reveals a low sintering level, under 900 °C, and the presence of visible dark-coloured areas reveals a sintering temperature over 1000 °C [23–25,28,29].

Table 1. Description of the specimens analysed in the study.

Clay Brick	Test Specimens	Origin	Production	Group	Microscopic Analysis [1]					
					T	*D*	*R*	*Df*	*I*	*C*
1	8	Toro	handmade	G1	<900 °C	y	n	n	y	n
2	15	Toro	handmade	G2	<900 °C	y	n	y	y	y
3	4	Toro	handmade	G3	>1000 °C	n	y	y	y	y
4	3	Toro	handmade	G3	>1000 °C	n	y	y	y	y
5	2	Toro	handmade	G2	<900 °C	y	y	n	y	y
6	8	Toro	handmade	G1	<900 °C	y	n	n	y	n
7	1	Toro	handmade	G2	<900 °C	y	y	n	y	y
8	2	Toro	handmade	G1	<900 °C	y	y	n	y	n
9	11	Entrala	handmade	G2	<900 °C	y	y	y	y	y
10	4	Otero Bodas	moulded	G3	>1000 °C	n	y	y	y	y
11	12	El Perdigón	moulded	G4	≥900 °C	n	y	y	y	y
12	11	El Perdigón	moulded	G4	≥900 °C	n	y	y	y	y
13	8	El Perdigón	extruded	G4	≥900 °C	n	y	y	y	y
14	6	El Perdigón	extruded	G4	≥900 °C	n	y	y	y	y
15	4	El Perdigón	moulded	G4	≥900 °C	n	y	y	y	y

[1] y: yes/n: no.

3. Experimental Analysis

3.1. Reception and Classification of Specimens

Dirt and remains of mortar were removed from clay bricks by sandpaper and metal brushes, as shown in Figure 2, to avoid contamination of the material. After that, bricks were numbered and catalogued recording their origin, characteristics and geometry. The elaborated register includes photographs to know the original shape of the specimens.

(**a**) (**b**) (**c**) (**d**)

Figure 2. Brick cleaning treatment (**a**) and cataloguing (**b**–**d**).

3.2. Preparation and Measurement of Test Specimens

Sampling of clay bricks was carried out by cutting, trying to extract the maximum number of specimens of the available material after removing grooves and superficial damages. As shown in Table 1, the number of test specimens extracted from each clay brick varies according to their size. A total of 102 specimens were tested, grouped into 15 series that correspond to the bricks of origin. In the extracting and conditioning operations, a STRUERS Labotom cutter with disc for ceramic cutting, a STRUERS LaboPol-1 brand polisher with 180 grit sandpaper, and a Memmerte brand dryer (T_{max} 350 °C) were used. The test specimens are parallelepiped, and their size is not uniform, with a height in the 13–33 mm range and a width in the 15–46 mm range. Although some bricks do not reach the minimum number of specimens required for compression tests according to the European Standard UNE EN 772-1: 2000 [32], the study considers all the results.

The samples are measured to obtain their apparent dry density (ρ_b), absorption (w_m), open porosity (π_a) and compressive strength (f_c), following the procedures outlined in Standards EN 772-13: 2001 [33], EN 771-1: 2003 [34] and EN 772-1: 2000 [32], as shown in Figure 3.

Figure 3. Measurement of the brick samples.

The lengths of the edges of the test specimens were obtained through a MITUTOYO CD 6" digital callipers of ±0.01 mm resolution. These measurements allow for the obtaining of the apparent volume (V_g), and the length and cross-sectional area (A_b) for compressive testing. Due to the difficulties of cutting, specimens do not satisfy the geometrical tolerances of European Standard EN 772-1: 2000 [32], so the study considers the average length of the four axial edges and the average cross-sectional area of the load faces.

The mass of the dry samples (m_d) and the mass of the wet samples, after one hour of immersion at 100 °C (m_w), were obtained by means of a KERN AIS-20-4N precision balance of 0.0001 gr resolution, a MICROTEST oven with programmable temperature controller Call 95000 P Process Controller, and a temperature-controlled PRECISTERM kettle, JP SELECT, Fuse (A) 8.

3.3. Dry Density, Absorption and Open Porosity

Based on the measurements previously discovered, the dry density (ρ_b) and absorption (w_m) of specimens are determined by Equations (1) and (2), according to Standards EN 772-13: 2001 [33] and EN 771-1: 2003 [34].

$$\rho_b = m_d / V_g, \quad (1)$$

$$w_m = (m_w - m_d)/m_d \times 100\%. \quad (2)$$

The open porosity (π_a), expressed as a percentage in volume, is obtained through Equation (3), where ρ_l corresponds to the density of the water at the tank temperature:

$$\pi_a = (m_w - m_d)/\rho_l/V_g \times 100\%. \quad (3)$$

Table 2 lists the average values and the coefficient of variation (CoV) of absorption, dry density and open porosity of each clay brick, calculated based on the experimental results of the specimens extracted from each brick. The average dry density of clay bricks ranges from 1225 kg/m^3 to 2193 kg/m^3. This difference is due to the various origins, manufacturing processes and deterioration, as in the case of clay brick number 7. Despite the differences between bricks, the results obtained from the specimens extracted from a clay brick show a low CoV, ranging from 0.36% to 3.54%, as seen in Table 2 and Figure 4a.

Table 2. Average values of the properties of the specimens from each clay brick and group.

Group	Clay Brick	$\overline{w_m}$ (%)	CoV w_m (%)	$\overline{\rho_b}$ (kg/m^3)	CoV ρ_b (%)	$\overline{\pi_a}$ (%)	CoV π_a (%)	$\overline{f_c}$ (N/mm^2)	CoV f_c (%)
	1	19	7.89	1577	2.59	31.0	6.38	9.5	55.69
	6	14	3.42	1832	1.06	25.9	3.13	23.6	16.92
	8	19	6.91	1570	0.51	31.2	7.60	12.1	2.40
G1		16	18.48	1687	7.60	28.49	10.71	15.5	53.23
	2	12	6.48	1904	1.22	23.5	5.39	17.5	26.14
	5	12	41.07	1954	0.36	24.0	40.92	18.3	22.79
	7	15	-	1225	-	19.2	-	9.2	-
	9	11	6.81	1854	1.49	21.1	5.95	13.7	18.62
G2		12	13.17	1853	7.31	22.3	12.31	15.9	29.26
	3	6	20.20	2193	1.79	12.8	18.94	61.7	23.69
	4	7	3.43	2069	0.90	14.6	4.15	64.4	15.91
	10	10	9.08	1889	1.61	19.8	8.81	45.1	34.40
G3		7	30.58	2044	6.84	15.5	23.31	55.6	30.63
	11	12	3.27	1919	1.18	23.4	3.06	24.0	27.04
	12	12	5.40	1876	3.54	24.3	5.07	20.6	13.5
	13	13	3.20	1894	1.59	25.0	3.01	13.2	18.28
	14	13	6.57	1875	1.12	26.0	5.53	12.9	22.52
	15	12	2.34	1946	0.45	24.0	2.64	22.6	33.47
G4		12	5.86	1894	2.34	24.45	5.05	19.37	34.62

w_m: absorption; ρ_b: dry density; π_a: open porosity; f_c: compression strength.

In general, the clay bricks from G1 present lower density mean values, while those from G3 record higher ones, as shown in Table 2 and Figure 5a. The results are related to their sintering level, presented in Table 1. Except for bricks 3 and 4, the density values are in the typical range for old bricks, between 1200 and 1900 kg/m^3 [35]. Finally, it should be noticed that the G4 specimens, manufactured in San Antonio Factory, have a very similar density among them, with a CoV of 2.34%.

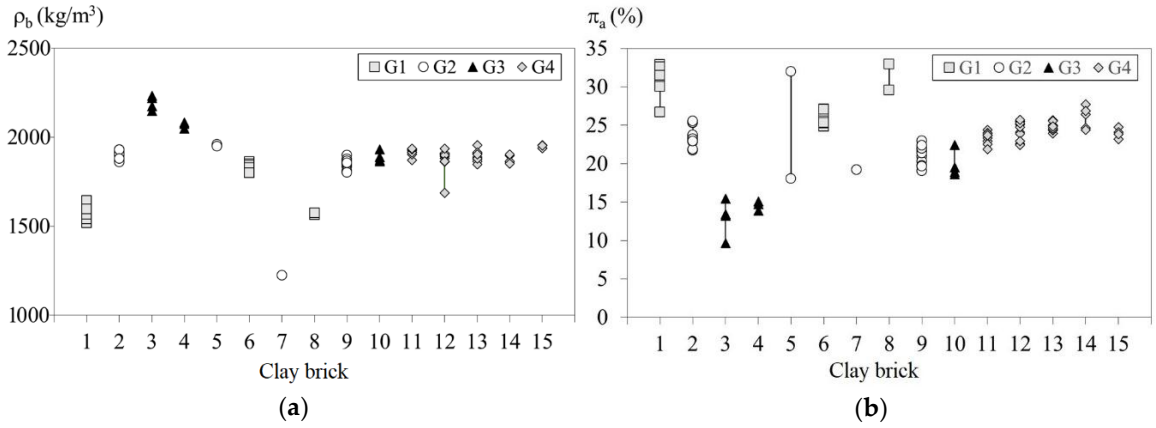

Figure 4. Results grouped by clay bricks: (**a**) dry density; (**b**) open porosity.

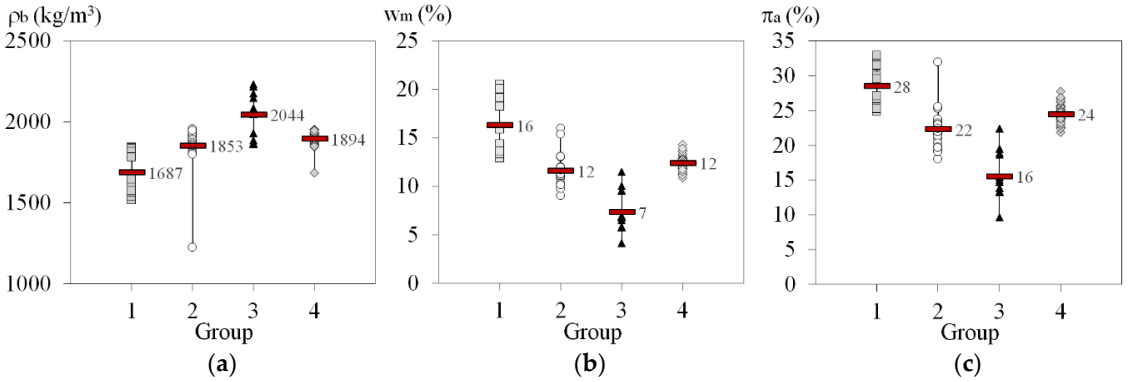

Figure 5. Results grouped by groups: (**a**) dry density; (**b**) absorption, (**c**) open porosity.

Porosity is an important parameter of clay bricks due to its influence on other properties [35]. As Fernandes et al. point in their work [35], historical clay bricks exhibit high porosity, ranging between 20% and 50%; only bricks 3 and 4 are outside of this range, with lower values in this case. The average results of open porosity and absorption vary significantly between bricks (see Table 2 and Figure 4b). Excluding brick 5, the open porosity of clay bricks exhibits low CoV compared with the old bricks analysed by Fernandes et al. [35], mainly in the case of bricks from G4. The clay bricks classified as G1 and G2 exhibit higher open porosity values (19.2–31.2%) and CoV, reaching 40.92%. In these two groups, the macroscopic analysis found larger defects, such as cracks between the phases and granular texture with large silica particles.

Absorption values, shown in Figure 5b, are in the typical range for old bricks, from 6% to 32% [35]. Since G1 has the highest absorption values, ranging from 13% to 21%, this group is the most vulnerable to moisture, predicting a strength drop in case of wet pieces [2].

3.4. Compressive Strength Test

The experimental analysis of the compressive strength were carried out using a universal electromechanical testing machine CODEIN MCO-30 model. Loading speed ranged between 0.12 and 0.89 $N/mm^2/s$, adjusted to the achieved strength, according to the European Standard EN 772-1: 2000 [32]. The compressive strength (f_c) is determined by dividing the maximum load (N_{max}) by the cross-sectional area of the pieces (A_b), affecting the ratio by a shape factor of δ, which depends on the geometry of specimens, as shown in Equation (4):

$$f_c = \delta\, N_{max}/A_b. \quad (4)$$

The small dimensions of the clay bricks, and therefore of the specimens obtained from them, prevent the use of the shape factor defined in European Standard EN 772-1: 2000 [32]. For this reason, according to the research of Caballero [36], the shape factor of ASTM C42/C42M-16 [37] is used. This factor is calculated based on the mechanical slenderness of the pieces. Due to their geometry, the specimens achieve mechanical slenderness values in the range from 0.41 to 1.13, but mostly under 1.

Figure 6 shows the compressive strength results of all tests. These results vary between clay bricks and between samples taken from the same brick. This is particularly the case in those that reach higher values of resistance. In addition, Figure 6 points out the average values of resistance of each brick, listed in Table 2. The average values are determined from the compressive strength results of the pieces whose slenderness is greater than 0.5, since below this value unpredictable resistance results are expected [38,39].

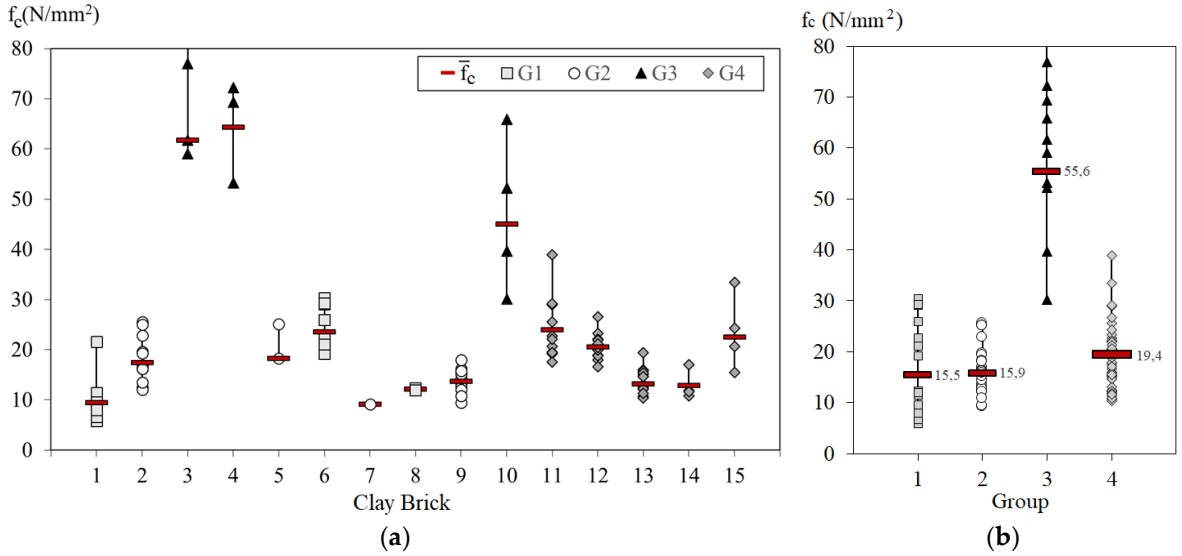

Figure 6. Compressive strength of (**a**) clay bricks and (**b**) groups.

4. Analysis of the Results

The average compressive strength of each brick exceeds 5 N/mm^2 in all cases—the minimum normalised compressive strength required according to Spanish Technical Building Code [21]—and ranges between 9.2 and 24.0 N/mm^2. The results are similar to those obtained in other comparable studies [8,11,13,16], except in the case of bricks of G3, in which the average strength is between 45.1 and 64.4 N/mm^2. Unusual strengths, higher than 50 MPa, were also reported by Pauri et al. [40]. Most studies on ancient clay bricks exhibit high CoV for compressive strength, ranging between 25% and 55% [35], as with most of the clay bricks in this study.

Figure 7 shows the correlation between compressive strength and open porosity, and between compressive strength and dry density, using all brick results. As shown in Figure 7a, the compressive strength of bricks is inversely correlated with open porosity. A linear fit with the equation $\pi_a = 27.9 - 0.18f_c$, provides an R^2 of 0.50. Due to the differences between clay bricks, a low correlation is obtained. Open porosity is related to the internal flaw, impurities and firing temperature, which significantly affect the compressive strength of the pieces. Due to the flow lines associated with the shaping process, clay bricks from G4 have a similar compressive strength to bricks with a low sintering level, from G1 and G2, as shown in Figure 6b. Clay bricks from G3 have open porosities ranging between 12% and 20%, much lower than in similar studies [7,9], an estimated sintering temperature up to 1000 °C, and therefore an unusual compressive strength.

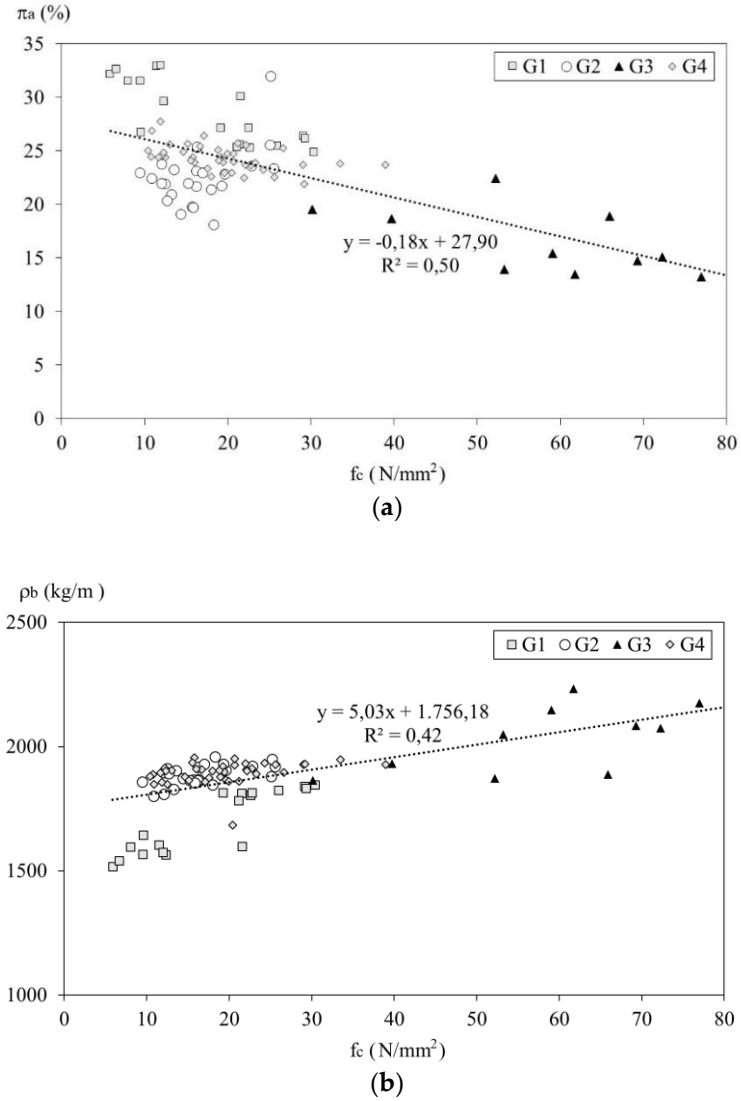

Figure 7. Correlations between the clay brick results: (**a**) open porosity-compressive strength and (**b**) dry density-compressive strength.

Figure 7b shows the relationship between the compressive strength of bricks and the dry density. A linear fit with the equation $\rho_b = 1756.18 + 5.03f_c$, provides an R^2 of 0.42. Removing the values from G1 bricks (poorly sintered), the correlation improves, providing an average R^2 value of 0.61.

5. Conclusions

This study analyses the physical properties and compressive strength of ancient clay bricks extracted from different buildings built in the 19th and 20th centuries in the province of Zamora (Spain). The visual inspection of clay bricks and their behaviour during the cutting process allowed to classify them into four groups and predict their physical and mechanical properties.

The results show that open porosity is the most significant physical characteristic for estimating the compressive strength of ancient clay bricks. Therefore, the visual inspection of the bricks can help us estimate the compliance with the minimum required compressive strength in samples that present a compact section with few pores or internal cracks.

Dry density values are directly related to the sintering process and have a positive correlation with the compressive strength of bricks. In this study, a high firing temperature, over 900 °C, and a high

density level, over 1700 kg/m^3, lead to compressive strength values of over 10 N/mm^2, as long as there are no cracks that cause failure.

Author Contributions: For research articles with several authors, a short paragraph specifying their individual contributions must be provided. The following statements should be used "Conceptualization, A.B.R.G., M.A.R.E., M.N.A.I., M.P.S.P. and M.S.C.O.; Methodology, A.B.R.G., M.A.R.E., M.N.A.I. and J.C.V.; Validation, A.B.R.G., M.A.R.E., M.N.A.I., M.P.S.P. and M.S.C.O.; Investigation, A.B.R.G., M.A.R.E., M.N.A.I. and J.C.V.; Writing-Original Draft Preparation, A.B.R.G.; Writing-Review & Editing, A.B.R.G., M.N.A.I., M.P.S.P.; Funding Acquisition, M.A.R.E., A.B.R.G., M.A.R.E., M.N.A.I., M.P.S.P. and M.S.C.O."

Funding: This research was funded by Fundación Memoria de Don Samuel Solorzano Barruso (Universidad de Salamanca) FS/18-2015.

Acknowledgments: Authors acknowledge the support given by GRUPO INZAMAC, in whose premises the compressive strength tests were carried out.

Conflicts of Interest: The authors declare no conflict of interest.

References

1. Binda, L.; Saisi, A.; Tiraboschi, C. Investigation procedures for the diagnosis of historic masonries. *Constr. Build. Mater.* **2000**, *14*, 199–233. [CrossRef]
2. Papayianni, I.; Stefanidou, M. Characteristics of bricks of Byzantine period. In *12th International Brick/Block Masonry Conference, Madrid, Spain, 25–28 June 2000*; Adell, J.M., Ed.; Construction and Architectonic Technology Department of the Polytechnic University of Madrid: Madrid, Spain, 2000; pp. 1729–1736.
3. Lourenço, P.B.; Fernandes, F.M.; Castro, F. Handmade clay bricks: Chemical, physical and mechanical properties. *Int. J. Archit. Herit. Conserv. Anal. Restor.* **2010**, *4*, 38–58. [CrossRef]
4. Brandonisio, G.; Luca, A.; Martino, A.; Mautone, G. Restoration through a Traditional Intervention of a Historic Unreinforced Masonry Building "Palazzo Scarpa" in Naples. *Int. J. Archit. Herit.* **2013**, *7*, 479–508. [CrossRef]
5. Vintzileou, E. Testing Historic Masonry Elements and/or Building Models. In *Perspectives on European Earthquake Engineering and Seismology. Geotechnical, Geological and Earthquake Engineering*; Ansal, A., Ed.; Springer: Berlin/Heidelberg, Germany, 2014; Volume 34, pp. 267–307, ISBN 978-3-319-07118-3.
6. Fernandes, F.; Lourenço, P.B. Evaluation of the Compressive Strength of Ancient Clay Bricks Using Microdrilling. *J. Mater. Civ. Eng.* **2007**, *19*, 791–800. [CrossRef]
7. Singh, S.B.; Munjal, P. Bond strength and compressive stress-strain characteristics of brick masonry. *J. Build. Eng.* **2017**, *9*, 10–16. [CrossRef]
8. Matysek, P.; Stryszewska, T.; Kańka, S.; Witkowski, M. The influence of water saturation on mechanical properties of ceramic bricks—Tests on 19th-century and contemporary bricks. *Mater. Constr.* **2016**, *66*, e095. [CrossRef]
9. Balasubramanian, S.R.; Maheswari, D.; Cynthia, A.; Balaji Rao, R.; Meher Prasad, M.; Goswami, R.; Sivakumar, P. Experimental determination of statistical parameters associated with uniaxial compression behaviour of brick masonry. *Curr. Sci. India* **2015**, *109*, 2094–2102. [CrossRef]
10. Azeez, O.; Ogundare, O.; Oshodin, T.E.; Olasupo, O.A.; Olunlade, B.A. Evaluation of the Compressive Strength of Hybrid Clay Bricks. *JMMCE* **2011**, *10*, 609–615. [CrossRef]
11. Pérez-Gálvez, F.; Rodríguez-Liñán, C.; Rubio, P. Determinación de las características mecánicas de los muros de fábrica de ladrillo en la arquitectura doméstica sevillana de los siglos XVIII Y XIX. *Inf. Constr.* **2009**, *61*, 19–28. [CrossRef]
12. Brozovsky, J.; Zach, J.; Brozovsky, J., Jr. Determining the strength of solid burnt bricks in historical structures. In Proceedings of the 9th International Conference on NDT of Art, Jerusalem, Israel, 25–30 May 2008.
13. Bajare, D.; Svinka, V.T. Restoration of the historical brick masonry. In Proceedings of the 9th International Congress on Deterioration and Conservation of Stone, Venice, Italy, 19–24 June 2000; pp. 3–11.
14. European Commission. *EN 1996-1-1: Eurocode 6: Design of Masonry Structures—Part 1-1: General Rules for Reinforced and Unreinforced Masonry Structures*; European Commission: Brussels, Belgium, June 2005.
15. Sahlin, S. *Structural Masonry. Englewood Cliffs*, 1st ed.; Prentice-Hall, Inc.: Upper Saddle River, NJ, USA, 1971.
16. Kaushik, H.B.; Rai, D.C.; Jain, S.K. Stress-strain characteristics of clay brick masonry under uniaxial compression. *J. Mater. Civ. Eng. ASCE* **2007**, *19*, 728–739. [CrossRef]

17. Lemos, J.V. Discrete Element Modeling of Masonry Structures. *Int. J. Archit. Herit.* **2007**, *1*, 190–213. [CrossRef]
18. Barbosa, C.S.; Lourenço, P.B.; Hanai, J.B. On the compressive strength prediction for concrete masonry prisms. *Mater. Struct.* **2010**, *43*, 331–344. [CrossRef]
19. Uday Vyas, C.V.; Reddy, B.V.V. Prediction of solid block masonry prism compressive strength using FE model. *Mater. Struct.* **2010**, *43*, 719–735. [CrossRef]
20. Sousa, R.; Sousa, H. Numerical simulations of masonry laboratory tests: A sensitivity analysis of the compressive behaviour. In Proceedings of the 15th International Brick and Block Masonry Conference, Florianopolis, Brazil, 3–6 June 2012.
21. Real Decreto 314/2006, de 17 de Marzo, por el que se Aprueba el Código Técnico de la Edificación. Available online: https://www.boe.es/buscar/act.php?id=BOE-A-2006-5515 (accessed on 3 April 2018).
22. Ley 8/2013, de 26 de junio, de Rehabilitación, Regeneración y Renovación Urbanas. Available online: https://www.boe.es/buscar/act.php?id=BOE-A-2013-6938 (accessed on 3 April 2018).
23. Spence, W.P.; Kultermann, E. *Construction Materials, Methods and Techniques. Building for a Sustainable Future*; Revised 1; Cengage Learning: Boston, MA, USA, 2016; p. 197. ISBN 978-1305086272.
24. Ingham, J. *Geomaterials under the Microscope. A Colour Guide*, 1st ed.; Manson Publishing, Academic Press: Devon, UK, 2013; pp. 163–164, ISBN 978-0-12-407230-5.
25. Kreimeyer, R. Some notes on the firing colour of clay bricks. *Appl. Clay Sci. Appl. Clay Sci.* **1987**, *2*, 175–183. [CrossRef]
26. Maniatis, Y.; Simopoulos, A.; Kostikas, A.; Perdikatsis, V. Effect of Reducing Atmosphere on Minerals and Iron Oxides Developed in Fired Clays: The Role of Ca. *Am. Ceram. Soc. Bull.* **1983**, *66*, 773–781. [CrossRef]
27. Arsenović, M.V.; Pezo, L.L.; Radojević, Z.M.; Stanković, S.M. Serbian heavy clays behavior: Application in rouch ceramics. *Hem. Ind.* **2013**, *67*, 811–822. [CrossRef]
28. Johari, I.; Said, S.; Hisham, B.; Bakar, A.; Ahmad, Z.A. Effect of the Change of Firing Temperature on Microstructure and Physical Properties of Clay Bricks from Beruas (Malaysia). *Sci. Sinter.* **2010**, *42*, 245–254. [CrossRef]
29. Cultrone, G.; Sidraba, I.; Sebastián, E. Mineralogical and physical characterization of the bricks used in the construction of the "Triangul Bastion", Riga (Latvia). *Appl. Clay Sci.* **2005**, *28*, 297–308. [CrossRef]
30. German, R.M. *Sintering Theory and Practice*, 1st ed.; Wiley-VCH: Weinheim, Germany, 1996; ISBN 978-0-471-05786-4.
31. Peters, T.; Iberg, R. Mineralogical changes during firing of calcium-rich brick clays. *Am. Ceram. Soc. Bull.* **1978**, *57*, 503–505.
32. Norma UNE-EN 772-1:2000. Métodos de Ensayo de Piezas para Fábrica de Albañilería. Parte 1: Determinación de la Resistencia a Compresión. Available online: https://www.aenor.com/normas-y-libros/normas (accessed on 3 April 2018).
33. Norma UNE-EN 772-13:2001. Métodos de Ensayo de Piezas para Fábrica de Albañilería. Determinación de la Densidad Absoluta seca y de la Densidad Aparente seca de Piezas para Fábrica de Albañilería. (Excepto piedra Natural). Available online: https://www.aenor.com/normas-y-libros/normas (accessed on 3 April 2018).
34. Norma UNE-EN 771-1:2003. Especificaciones de Piezas para Fábrica de Albañilería. Parte 1: Piezas de Arcilla Cocida. Available online: https://www.aenor.com/normas-y-libros/normas (accessed on 3 April 2018).
35. Dan, M.B.; Přikryl, R.; Török, Á. *Materials, Technologies and Practice in Historic Heritage Structures*; Stringer Science + Business Media B.V.: Berlin/Heidelberg, Germany, 2009.
36. Caballero Valdizán, J.M. Aprovechamiento y Reciclaje de Residuos de Construcción y Demolición Mediante Técnicas de Sinterización. Ph. D. Thesis, University of Salamanca, Zamora, Spain, 2017.
37. ASTM International. *ASTM C42/C42M—16 Standard Test Method for Obtaining and Testing Drilled Cores and Sawed Beams of Concrete*; ASTM International: West Conshohocken, PA, USA, 2016.
38. Murdock, J.W.; Kesler, C.E. Effect of Length to Diameter Ratio of Specimen on the Apparent Compressive Strength of Concrete. *ASTM Bull.* **1957**, *221*, 68–73.

39. Celik, A.O.; Kilinc, K.; Tuncan, M.; Tuncan, A. Distributions of Compressive Strength Obtained from Various Diameter Cores. *ACI Mater. J.* **2012**, *109*, 597–606.
40. Pauri, M.; Stazi, A.; Mastrosanti, F.; D'Orazio, M. The decay of ancient building masonry, a case study. In Proceedings of the 10th International Brick/Block Masonry Conference, Calgary, AB, Canada, 5–7 July 1994; pp. 1295–1304.